Currents with underwater porous obstacles

Umurdin Dalabaev[1,*], and *Nusratilla* Latipov[2]

[1]University of World Economy and Diplomacy, 100007 Tashkent, Uzbekistan
[2]National University of Uzbekistan, 100174 Tashkent, Uzbekistan

Abstract. The work is devoted to the flow of incompressible fluid in an open flow with porous obstacles (vegetation, hill). For mathematical modeling of such flows, a single equation of suitability in the porous and free zone is used. The model is based on Rakhmatulin's two-speed model. Numerical results of the hydrodynamic features of a two-dimensional viscous flow are presented. In the free zone, the equation turns into the Navier-Stokes equation, and in the porous region, into the Darcy-Forchheimer equation. For the numerical solution, the SIMPLE algorithm was used.

1 Introduction

In many environmental and technical processes, porous media play a major role in fluid flow. The main parameters controlling the flow of liquid with porous barriers are the permeability and porosity of the medium. Especially in channel flows, interactions of the fluid flow with various porous inclusions are observed: flow in the presence of sediment, with vegetation, with an uneven bottom, etc. The study of flow patterns in the combined region is one of the areas of research in the field of mechanics of multiphase media [1-9].

There are two approaches to modeling the flow of liquid or gas in areas with porous inclusions. In the first approach, the free zone is modeled by the Navier-Stokes equation; in the porous region, various equations such as Darcy, Brinkman, etc. Various boundary conditions are applied to the interior boundary to represent free flow filtration through the porous media. The Beavers–Joseph or Safman conditions are used as interboundary conditions [1-5,12-15].

In the second approach, the flow is modeled for the entire region by a single equation, without identifying the interphase boundary. The second approach is more realistic in terms of the numerical implementation of the algorithm [10,11,16-21].

This work represents a further development of the application of the two-speed model [17-21] for new tasks. Knowledge of hydrodynamic fields allows for further study of the entrainment and deposition of particles at the bottom of the channel.

* Corresponding author: udalabaev@mail.ru

2 Mathematical model and numerical method

Let us consider an interpenetrating model that describes the flow of two-phase media [8-9], where the velocity of the discrete phase is neglected. Then the flow of the liquid phase is described by a system of equations (two-dimensional case):

$$fu\frac{\partial u}{\partial x}+fv\frac{\partial u}{\partial y}=-\frac{f}{\mathrm{Re}}\frac{\partial p}{\partial x}+\frac{4}{3\mathrm{Re}}\frac{\partial}{\partial x}\left(f\frac{\partial u}{\partial x}\right)+$$
$$+\frac{1}{\mathrm{Re}}\frac{\partial}{\partial y}\left(f\frac{\partial u}{\partial y}\right)-\frac{2}{3\mathrm{Re}}\frac{\partial}{\partial x}\left(f\frac{\partial v}{\partial y}\right)+\frac{1}{\mathrm{Re}}\frac{\partial}{\partial y}\left(f\frac{\partial v}{\partial x}\right)-Cu-\frac{\sin\alpha}{Fr}, \quad (1)$$

$$fu\frac{\partial v}{\partial x}+fv\frac{\partial v}{\partial y}=-\frac{f}{\mathrm{Re}}\frac{\partial p}{\partial y}+\frac{1}{\mathrm{Re}}\frac{\partial}{\partial x}\left(f\frac{\partial v}{\partial x}\right)+$$
$$+\frac{4}{3\mathrm{Re}}\frac{\partial}{\partial y}\left(f\frac{\partial u}{\partial y}\right)+\frac{1}{\mathrm{Re}}\frac{\partial}{\partial x}\left(f\frac{\partial v}{\partial y}\right)-\frac{2}{3\mathrm{Re}}\frac{\partial}{\partial y}\left(f\frac{\partial v}{\partial x}\right)-Cv.-\frac{\cos\alpha}{Fr}, \quad (2)$$

$$\frac{\partial(fu)}{\partial x}+\frac{\partial(fv)}{\partial y}=0 \quad (3)$$

Here, $u, v-$ longitudinal and transverse flow velocities, $p-$ pressure, f volume concentration, Re is Reynolds number, C is interaction coefficient. In equations (1-3) the parameters are dimensionless (Re=$UH\rho/\mu$), U is the average volume velocity, L is the characteristic scale, $\rho-$ is the density of the liquid, μ is the viscosity, H is channel height). The Kozeny-Karman relation was used for the interaction coefficient: $C=\frac{D^2}{\mathrm{Re}}\frac{(1-f)^2}{f^2}+0.55D\sqrt{f}(1-f)\sqrt{u^2+v^2}$, $D=\sqrt{\beta}H/d$, where d is the characteristic size of the porous medium. Fr is the Froude number, α is the angle of inclination to the horizon, β is the coefficient in the Kozeny-Karman formula.

Equations (1)-(3) make it possible to study flows both inside and outside a porous medium, since at f = 1 we obtain the Navier-Stokes equations for an incompressible fluid. Moreover, these equations are suitable for the entire region under consideration. To numerically solve (1)-(3), we use the control volume method [20,21] with a non-uniform mesh. The uneven mesh was built so that their concentrations formed around the porous medium. The SIPMLE algorithm [20] is generalized for equations (1)-(3).

3 Results and discussion

3.1 Flow around underwater vegetation

The flow area and the direction of the coordinate axis with vegetation are presented in Fig.1. Equation (1)-(3) is considered in the area: $0\le x\le L,\ 0\le y\le 1.$ (L=4). The vegetation consists of two tufts. Vegetation size: width 0.5 and height 0.3, the distance between a bunch of vegetation is 0.5.

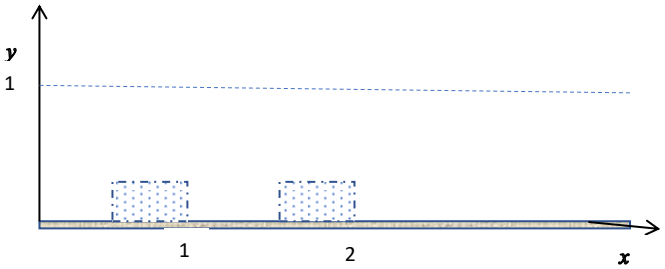

Fig.1. Flow region and direction of axes.

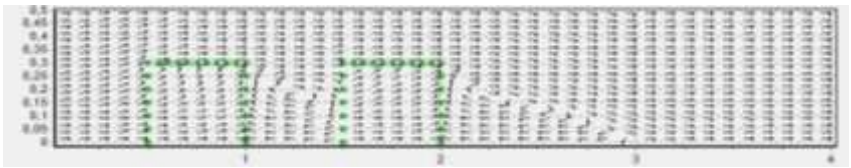

a) f=0.8,

b) f=0.5

c) f=0.1

Fig. 2. Current velocity field. *Re*-100, *D*=1000, *Fr*=0.5.

For clarity, the figures show that part of the channel where the flow undergoes severe deformation.

Figure 2 shows the flow field with flow parameters: *Re*=100, *D*=1000, *Fr*=0.5, sinα=0.0001. A comparison of Fig.2 shows that the flow pattern near porous barriers is similar, but inside it differs significantly.

Figure 3 shows the direction of the velocity field at various porosities at *Re*=200, *D*=1000, *Fr*=0.5, sinα=0.0001.

Figure 3 shows the strong dependence of the recirculation flow behind the second part of the porous barrier for all porosities.

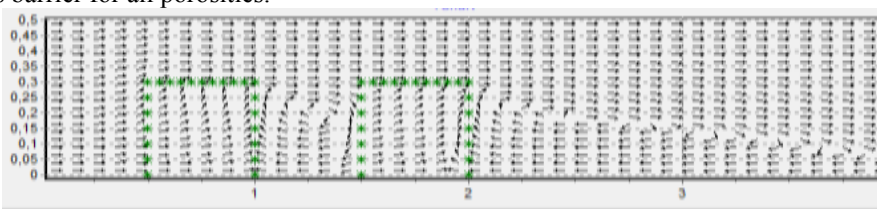

a) f=0.8

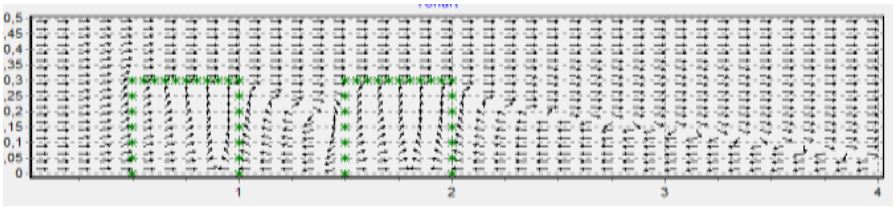

b) f=0.5

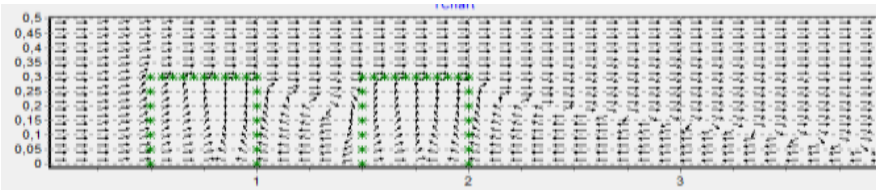

c) f=0.1

Fig. 3. Current velocity field. *Re*-200, *D*=1000, *Fr*=0.5.

In both cases, at high porosities, the flow inside the porous barriers coincides with the external flow. With increasing Reynolds number, the synchronization of flow inside and outside porous media is disrupted (compare Fig.2b) and Fig.3b)).

3.2 Problem of flow around a porous hill

Let part of the open channel be filled with a porous layer. Equation (1)-(3) is considered in the area: $0 \le x \le L,\ 0 \le y \le 1.$ The x axis is directed along the lower wall of the channel, and the y axis is perpendicular to it. Upon entering the channel, a parabolic velocity profile is given. Part of the channel is filled with a porous layer: $0,5 \le x \le 1.5,\ 0 \le y \le g(x)$ $\left(g(x) = \frac{h_0}{2}\left[1 + \cos\frac{2\pi}{L_0}\left(x - d - \frac{L_0}{2}\right)\right]\right)$, here d is the distance from the entrance to the channel, h_0 is the fullness of the channel, L_0 is the width of the porous layer.

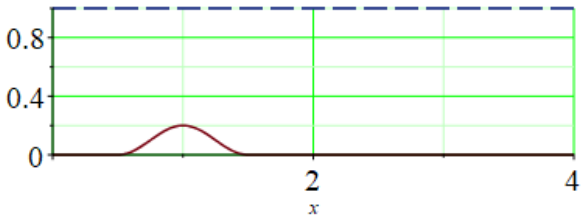

Fig. 4. Flow region with porous hill.

At the boundaries of the computational domain, a no-slip condition is specified on the solid wall; hydrostatic pressure and Poiseuille flow are specified at the channel inlet; and at the output - a soft boundary condition. On the free surface we use the boundary condition:

$$\frac{\partial u}{\partial y} = 0,\ v = 0.$$

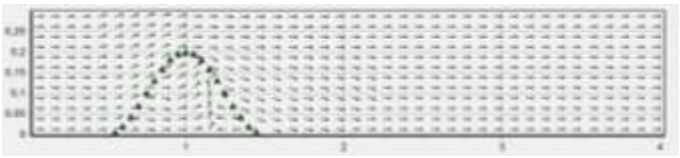

a) direction of the velocity field (part of the region) f=0.8;

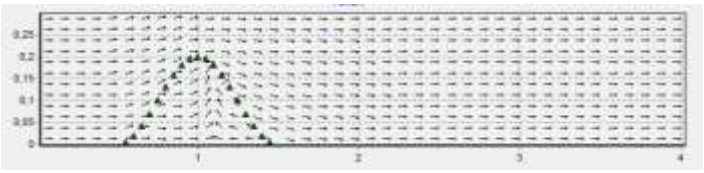

b) direction of the velocity field (part of the region) f=0.5

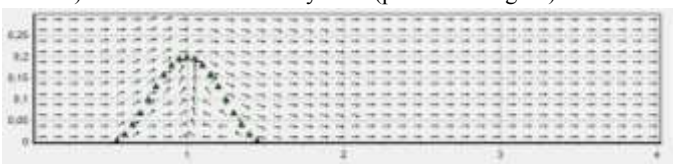

c) direction of the velocity field (part of the region) f=0.1

Fig. 5. Calculation parameters: *:Fr*=0.5, *D*=1000; *Re*=100; L=4; *h*0=0.5; L0=1; *d*=0.2; sinα=0.000001

In Fig.5 the direction of the velocity field is presented. Outside the porous layer, the direction of the layer field does not depend on porosity. Inside the porous layer, an asymmetry in the direction of the velocity field is observed, while a decrease in porosity leads to a symmetrical field direction inside the porous layer.

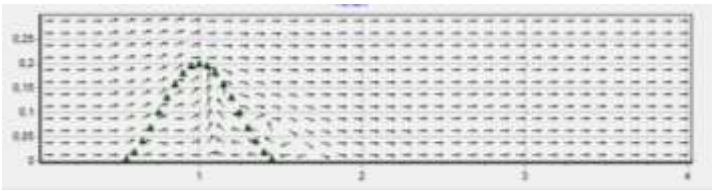

a) direction of the velocity field Re=200

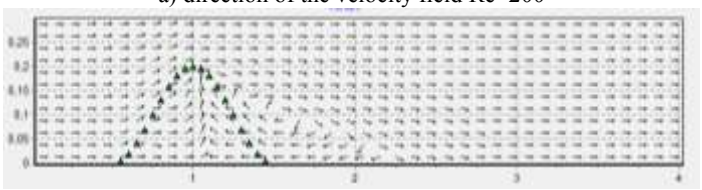

b) direction of the velocity field Re=500

Fig. 6. Calculation parameters: :*Fr*=0.5, *D*=1000; *f*=0.5*; L*=4; *h*0=0.5; *L*0=1; *d*=0.2; sinα=0.000001

In Fig.6 the influence of the Reynolds number on the field and the direction of the current is given. Increasing the Reynolds number will lead, on the one hand, to the appearance of secondary currents behind the hill, and on the other, to an expansion of the zone of influence of circulation currents.

4 Conclusion

Using the proposed model, which is obtained on the basis of a two-speed interpenetrating model, it is possible to obtain a characteristic of the hydrodynamic fields of joint flow with

porous inclusions. The extended Navier-Stokes model can be used to study hydrodynamic structures for flow in complex regions using a single equation without explicitly identifying the interregional boundary.

References

1. D. A. Nield, A. Bejan, *Convection in Porous Media* (Springer International Publishing AG, 2017)
2. M. Ehrhardt, An Introduction to Fluid-Porous Interface Coupling, Progress in computational physics **2**, 3–12 (2000)
3. F. A. Moralesa, R. E. Showalterb, J. Math. Anal. Appl. **452**, 1332–1358 (2017)
4. J. A. Ochoa-Tapia, S. Whitaker, J. Porous Media **1**, 201–217 (1998)
5. P. Yu, T. S. Zeng, Y. Low, Y. T., Int. J. Numer. Meth. Fluids **53**, 1755-1775 (2006)
6. M. A. Gol'dshtik, *Protsessy perenosa v zernistom sloye* (Institut teplofiziki SO AN SSSR, Novosibirsk, 1984)
7. V. A. Kirillov, V. A. Kuz'min, V. I. P'yanov, V. M. Khanayev, DAN SSSR **245(1)**, 159-162 (1979)
8. D. F. Faizullaev, *Laminar Motion of Multiphase Media in Conduits* (Springer US, 1969)
9. R. I. Nigmatulin, *Fundamentals of the mechanics of heterogeneous media* (Izdatel'stvo Nauka, Moscow, 1978)
10. F. Cimolin, M. Discacciati, Applied Numerical Mathematics **72**, 205-224 (2013)
11. F. J. Vald_es-Parada, D. Lasseux, Phys. Fluids **33**, 022106 (2021)
12. Ye. V. Mosina, I. V. Chernyshev, Techeniye zhidkosti v ploskom kanale nad sloyem regulyarnoy poristoy sredy
13. P. V. Bulat, K. N. Volkov, Industrial and Systems Engineering **34(3)**, 283 – 300 (2020)
14. I. I. Potapov, K. S. Snigur, G. I. Tsoy, Vychislitel'nyye tekhnologii **24(6)**, 99–107 (2019)
15. K. B. Tsiberkin, Computational continuum mechanics **11(4)**, 438-447 (2018)
16. S. V. Polyakov, M. A. Trapeznikova, A. G. Churbanov, N. G. Churbanova, Preprints of the Institute of Mechanical Engineering named after. M. V. Keldysh **71**, 19 (2021)
17. U. Dalaboyev, Inzhenerno-fizicheskiy zhurnal **70(3)**, 390-394 (1997)
18. U. Dalabaev, Turkish Journal of Physics **21(5)**, 649-356 (1997)
19. U. Dalabaev, Journal of Engineering Physics and Thermophysics **84(6)** (2011)
20. U. Dalabaev, AIP Conference Proceedings **2365**, 060015 (2021)
21. U. Dalabaev, N. Latipov, E3S Web of Conferences **431**, 04017 (2023)
22. S. Patankar, *Numerical Heat Transfer and fluid Flow* (1980)
23. J. Blazek, Computational Fluid Dynamics: Principles and Applications (Elsevier, 2001)